International Journal of Interdisciplinary Innovative Research &Development (IJIIRD)

ISSN: 2456-236X

Vol. **04** Issue **02** |**2020**

A Hybrid Approach to Improve the Clipping Technique of PAPR Reduction in OFDM

Mohammed Zakee Ahmed[1], Sayyad Ajij D[2]

[1]*Assistant Professor, Department of E&TC,PICT Pune, MS, India*
[2]*Vice Principal, MIT Aurangabad, MS, India*

ABSTRACT

The most vulnerable characteristics of Orthogonal Frequency Division Multiplexing (OFDM) signal is a High Peak to Average Power Ratio (PAPR). Being one of the used PHY standards, OFDM has broad scope in future wireless networks. PAPR directly affects the performance of OFDM based systems. Numerous authors have proposed plenty of methods of PAPR reductionsviz: interleaving (INT), Selective Mapping (SLM), Partial Transmit Sequence (PTS), and Many more. However, most of the method degrades Bit Error Rate (BER) performance or increases computational complexity. One of such least complexity method is Amplitude clipping and Filtering (ACF). Amplitude clipping is merely restricting the signal amplitude to not to exceed a threshold value. This threshold value is decided based on the minimum requirement of signal reconstruction. In this paper, we have proposed a technique where we have tested various threshold values of amplitude clipping ranging to hyper level, which is approximately very near to the average power of the OFDM signal. The OFDM signal is preprocessed before clipping it so that BER degrades as minimum as possible. Thus, by applying a modified least complexity PAPR reduction technique, we can get better PAPR and BER control. The OFDM signal is designed here is based on the 802.11a IEEE WLAN standard. The framework is designed to test the PAPR reduction algorithm using the LabVIEW tool. This framework fundamentally constructs the OFDM signal right from binary sequence to final OFDM baseband signal. The validation of this baseband signal done through a Wireless network Testbed of NI- USRP2922 Software Defined Radio Platform. The present paper illustrated all the modeling and implementation process, along with achieved results.

Keyword: OFDM, PAPR, IEEE802.11a, LabVIEW, NI-USRP

1. INTRODUCTION

In the context of signal design, an OFDM signal is simply a mapping of input complex constellation symbols onto the orthogonal set of subcarriers realized by IFFT. In addition to input complex constellation symbols, some symbols are intentionally added to serve synchronization (Reference Symbols), to deal with multipath effects (Cyclic Prefix) and to match with IFFT Size (Zero Padding) [1-5].

The Mathematical form of an OFDM [1-5] baseband signal is as depicted in Equation 1.

$$s_q(t) = \sum_{p=0}^{N-1} X_{p,q}\, \phi_p(t - qT) \qquad (1)$$

Where q is the OFDM symbol number
$X_{p,q} = [X_{0,q}, X_{1,q},\ldots,X_{N-1,q}]$ are complex number symbols from a set of signal constellation points, $\{\Psi\}$.
Equation 1 can again simplify as

$$s_{r,q} = \frac{1}{\sqrt{N}} \sum_{p=0}^{N-1} X_{p,q}\, e^{j\,2\pi \frac{r}{N} p} \quad \begin{matrix} 0 \le r \le N-1 \\ 0 \le p \le N-1 \end{matrix} \qquad (2)$$

The $s_{r,q} = [s_{0,q}, s_{1,q},\ldots,s_{N-1,q}]$ are carrier amplitudes associated with the OFDM symbol. As depicted in equation 2, it is a formal expression for IFFT, $\mathfrak{F}^{-1}\{X_{p,q}\}$. Equation 3 depicts an infinite sequence of OFDM symbols to be transmitted.

$$s(t) = \sum_{q=-\infty}^{\infty} s_q(t) = \sum_{q=-\infty}^{\infty} \sum_{p=0}^{N-1} X_{p,q}\phi_p(t - qT) \quad (3)$$

Adjacent subcarriers of an OFDM signal are said to be orthogonal if their cross product is zero; thus, orthogonality is simply a mathematical relationship that shows the disjoint nature of two adjacent subcarriers. It can be precisely described with equation-4 and Figure 1.

$$\int_0^T \psi_p(t)\psi_{p'}^*(t)\,dt = \begin{cases} \delta(p - p') & p = p' \\ 0 & \text{otherwise} \end{cases} \quad (4)$$

Where ψ is representing the signal set. δ [.] is the delta function, and (.)* is its complex conjugate.

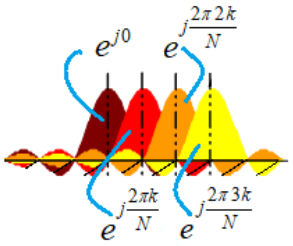

Fig-1 Mutually Orthogonal Subcarriers

The fundamental construction of the OFDM signal is made according to figure 2, and then it is tested on Universal Software Radio Peripheral NI-USRP2922 [6]. The testbed is shown in figure 3. For validation of this signal, The IEEE WLAN 802.11a network specifications followed here is as depicted in Table 1 [7].Input symbols are arranged according to specifications given in Table 1. Additional symbols are merged into these input symbols for the sake of synchronization channel estimation minimizing multipath effect and matching the IFFT size. This sample/symbol arrangements form one OFDM symbol, as illustrated finely in figure 4 [2].

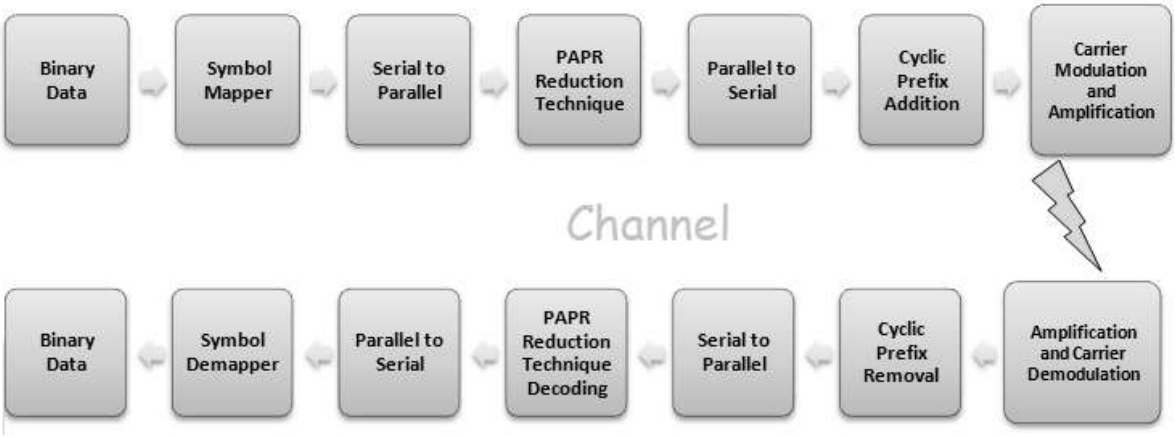

Fig-2 Block Diagram OFDM Tx Rx

In the conventional OFDM Tx-Rx block diagram, in place of PAPR reduction technique and decoding, the IFFT and FFT blocks are deployed, respectively.One OFDM symbol of total 52 subcarriers, out of that 48 are data subcarriers 4 are pilot subcarriers. A total of 12 zeros are padded at the upper and lower end to reduce adjacent channel interference. These 64 frequency-domain symbols are transformed with IFFT to time-domain symbols. The last

eight symbols are prefixed, making 72 symbols in one OFDM Symbol. The zero-padding is a procedure wherein OFDM symbol, the first 6 location, center, and last five locations zeros are inserted, making output symbol count 64 so that the 64-IFFT operation can be performed [7]. After IFFT, the symbols will become time domain values. The CP is realized by adding the last eight vales of these time-domain values into the beginning of the symbol, making the total symbol count 72. These 72 symbols are called s IQ data, the 'I' represent the magnitude, and 'Q' represents phase values. These IQ values are upconverted with the sine and cosine waves of frequency, defined in WLAN standard, and integrated into one signal representing one OFDM symbol [9].

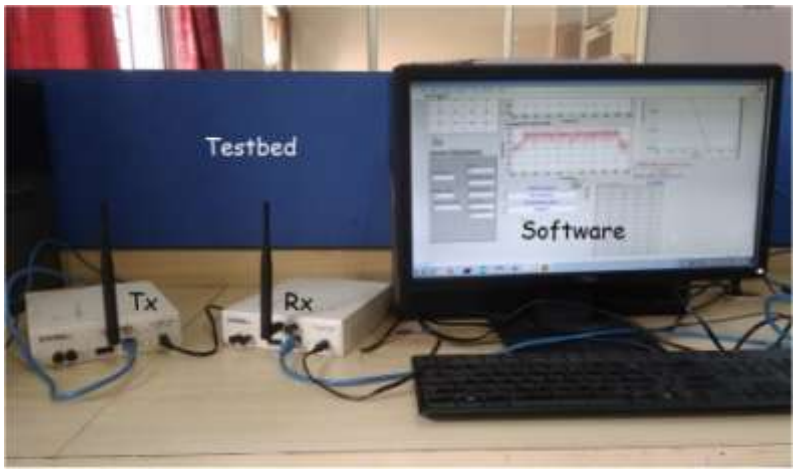

Fig- 3 Testbed setup with NI-USRP 2922

Table-1 WLAN 802.11a Specifications

Terms	Specific Value
$N_{SD} - Data\ Subcarriers$	48
$N_{SP} - Pilot\ Subcarriers$	4
N_{ST} $- Total\ Number\ of\ Sabcarriers$	52
$\Delta F - Frequence\ Spacing$	0.3152MHz
$T_{FFT} - FFT\ Period$	3.2 μs
$T_{CP} - Cyclic\ Prefix\ Duration$	0.8 μs
$T_{Sym} - Symbol\ Duration$	4.0 μs
$FFT\ Size$	64
$Modulation\ Scheme$	BPSK, 4QAM, 16QAM, 64QAM

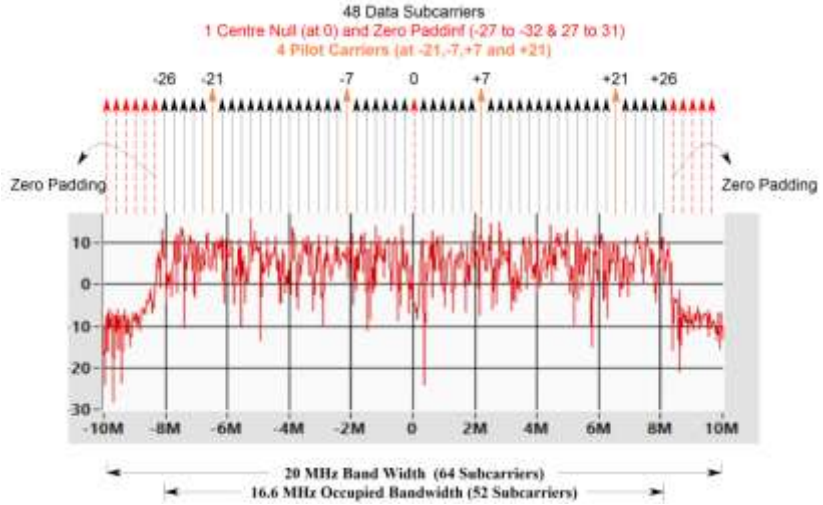

Fig- 4.WLAN 802.11 OFDM Symbol Structure

1.1 The PAPR: The primary reason for High PAPR in an OFDM signal is the alignment of subcarriers having the same phase, which is measured in terms of the difference between peak power and average power of the signal. PAPR in dB is measured with [4][5]

$$PAPR_{dB} = 10\, log_{10}(PAPR)$$

Mathematically it is defined as given in equation 5

$$\xi = \frac{\max_{\forall\, q,r\in[0,N-1]} |s_{r,q}(t)|^2}{\mathrm{E}\left\{|s_{r,q}(t)|^2\right\}} \qquad (5)$$

Where E{·} represents the statistical expectation
The uncertain values of PAPR make the transmitter high power amplifier (HPA) unstable. Choosing a wideband HPA increases the cost of the system; this expense will be a waste as a high peak in signal is probably may occur less frequently.[4] Thus, the HPA is to be operated in the low power efficiency regime to prevent this expense. It may directly affect the battery life in most of the handheld devices. High PAPR may cause loss of all the substantial benefits of OFDM systems. By controlling high PAPR, the HPA Efficiency can be improved in the transmitter, and the signal distortion and increased BER due to HPA nonlinearity can be optimized. The most significant achievement of PAPR reduction is, up to 9% of the transmission power can be saved by just reducing 1 dB of PAPR [8]. Several PAPR reduction techniques referred for system implementation viz ACF [10-13], INT [14-17], SLM [18-21], and PTS [22-25].

2. SYSTEM IMPLEMENTATION

The conventional ACF Technique [10-13] clips the concerning high peak amplitudes of the time-domain signal following the value of Clipping Threshold (CT), filters the signal in the frequency domain, and repeats both the step in a loop for a defined number of times. The CT, represented by symbol 'A' here, that decides the threshold amplitude value above which the signal is clipped. Figure 5 shows the ACF block diagram; the clipping can be represented with the following equation

$$x(t)_{\text{clipped}} = \begin{cases} x(t) & |x(t)| < A \\ Ae^{j\theta(t)} & |x(t)| > A \end{cases} \qquad (6)$$

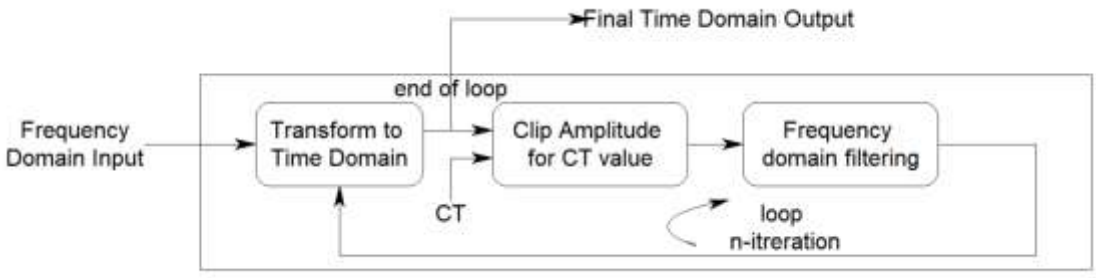

Fig. 5. Block Diagram of ACF

The input frequency domain symbols are time converted with IFFT, and then by comparing all the symbols one by one, all are evaluated to their amplitude values, amplitude exceeding to the threshold value is simply clipped off by replacing it with$Ae^{j\theta(t)}$ as shown in equation-6. Here equation-6 does not represent frequency domain filtering. All the symbols collected are processed with FFT later, as frequency-domain filtering. The number of peaks clipped will decide the signal degradation at the receiver due to the loss of valuable information.

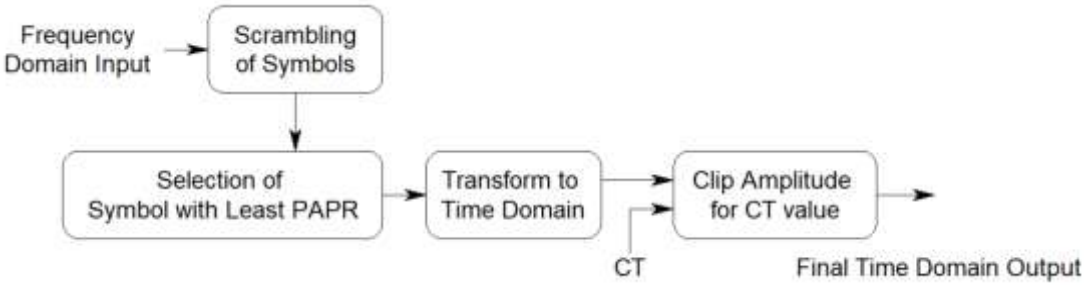

Fig. 6. Proposed PAPR Reduction Technique

We have tested a method where before the clipping signal is preprocessed. The signal is scrambled with a lightweight multiplication of unique phase vectors to scramble the symbols; this scrambling will shuffle the symbol position, and summing of similar phase sequences may be avoided by testing different combinations. This processed signal then later is clipped with equation 6. The block schematic of the proposed method is as shown below [26-28]. Mathematically the overall operation is briefed as follows

The input frequency symbols $x = [x_0, x_1, x_2, \dots x_{N-1}]$ pointwise multiplied with M different phase factors$b_m = [b_m^0, b_m^1, b_m^2, \dots b_m^{N-1}]$. This point multiplication is done along with IFFT,$X_m^n = \sum_{n=0}^{N-1} x_n \, b_m^n \, e^{j\frac{2\pi nt}{N}}$

$$X_{prepro} = \underset{m=0,1,2,..M-1}{\arg} min_{X_m^n} \left(\max_{n=0,1,2,..N-1} |X_m^n| \right) \quad (7)$$

$$\check{X} = \underset{m=0,1,2,..M-1}{\arg} min_m \left(\max_{n=0,1,2,..N-1} |X_m^n| \right) \quad (8)$$

$$x_{Hybrid} = \begin{cases} x_{prepro} & |x_{prepro}| < A \\ Ae^{j\theta(t)} & |x_{prepro}| > A \end{cases} \quad (9)$$

Here value of ***A is varied from 0.15 to 0.18***,wherethe peak value is observed 0.22.

3. RESULTS AND DISCUSSION

In the following section, with (a) and (b) of Figures 7, 8, 9, and 10, ACF and the proposed techniques are comparative analyzed. This comparison is highlighted in (a) and (b) of figure 7. Here the constellation diagrams, max PAPR value, Complementary Cumulative Distribution Function (CCDF), and Bit Error Ratio Vs. The ratio of Energy/Bit (Eb) to the Spectral Noise Density (N0) (Eb/N0) is compared of both the techniques. As shown in Figure 7 shows the proposed technique with clipping threshold 0.15, it is preventing 0.4 dB in CCDF rise and 3 dB in BER vs. Eb/N0 rise. As shown in the results of figure 8, it can be observed that with clipping threshold 0.16 the proposed technique is preventing 0.4 dB in CCDF rise and 2 dB BER vs. Eb/N0 rise. With Figure 9 the proposed technique results can be observed for clipping threshold 0.17it is preventing 0.3 dB in CCDF rise and 1 dB in BER vs. Eb/N0 rise. Finally as shown in the results of figure 10, it can be observed that with clipping threshold 0.18 the proposed technique is preventing 0.3 dB in CCDF rise and 1 dB in BER vs. Eb/N0 rise.

The Signal Constellations observed in ACF Technique is moderately spread, and in Proposed, Technique confined in all the results. The detailed summary comparison is illustrated by Table 2 Where it shows CCDF values in dB and BER vs. Eb/N0 in dB.

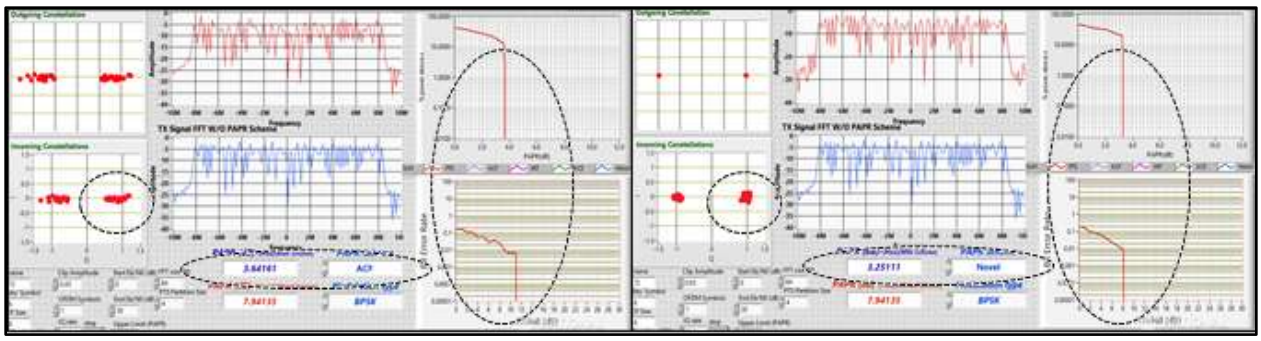

a) (b)

Fig- 7: LabVIEW Front Panel of (a) ACF (b) Proposed for CR=0.15

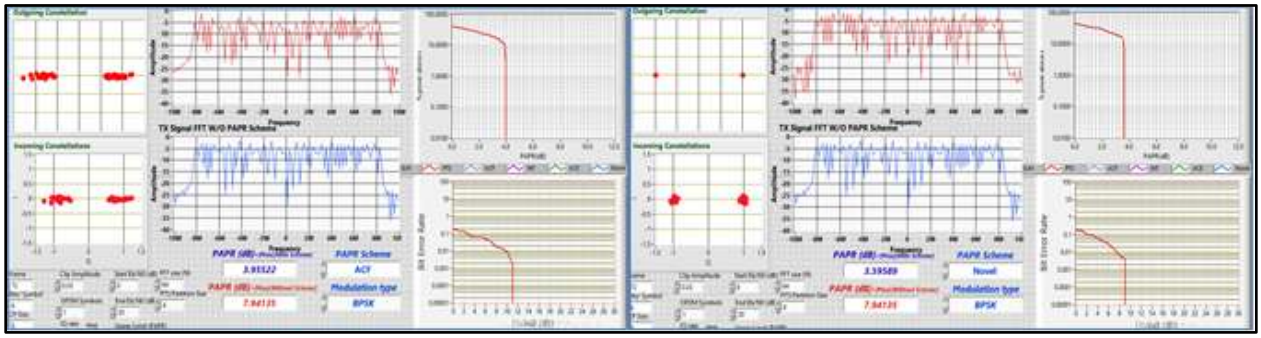

(a) (b)

Fig- 8: LabVIEW Front Panel of (a) ACF (b) Proposed for CR=0.16

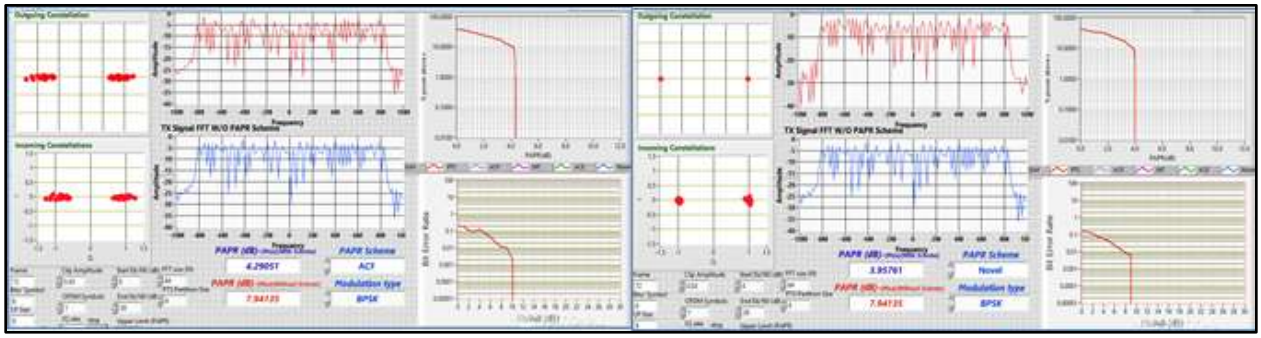

(a) (b)

Fig- 9: LabVIEW Front Panel of (a) ACF (b) Proposed for CR=0.17

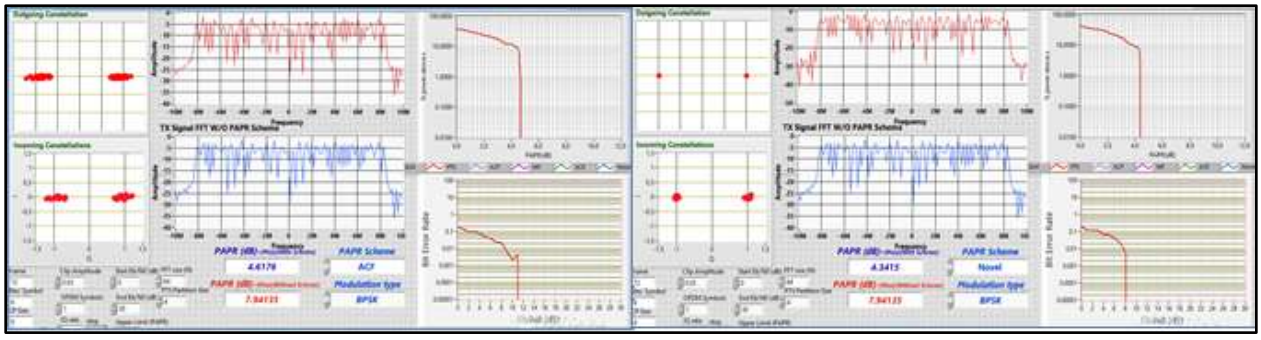

(a) (b)

Fig- 10: LabVIEW Front Panel of (a) ACF (b) Proposed for CR=0.18

Table-2:CCDF and BER Vs EB/N0 values of ACF and Proposed method for Clipping Threshold 0.15, 0.16, 0.17 and 0.18

Clipping Thresholds		PAPRReductionTechnique	Modulation Techniques			
			BPSK	4-QAM	16-QAM	64-QAM
CT=0.15	CCDF	ACF	3.6	3.2	3.2	4.1
		Proposed	3.2	3	3	3.8
	BER vs. Eb/N0	ACF	11	20	27	35
		Proposed	8	18	21	35
CT=0.16	CCDF	ACF	4	3.6	3.6	4.5
		Proposed	3.6	3.4	3.4	4.2
	BER vs. Eb/N0	ACF	11	20	24	35
		Proposed	9	18	20	30
CT=0.17	CCDF	ACF	4.3	4	4	5
		Proposed	4	3.8	3.8	4.6
	BER vs. Eb/N0	ACF	10	20	22	35
		Proposed	9	18	19	29
CT=0.18	CCDF	ACF	4.6	4.4	4.4	5.3
		Proposed	4.3	4.2	4.1	5
	BER vs. Eb/N0	ACF	11	18	22	31
		Proposed	8	17	19	28

4. CONCLUSIONS

The conventional scrambling techniques have high computational complexities and the conventional Amplitude Clipping method has high BER. The optimum solution can be achieved with proposed technique where, the computational complexity is controlled me reducing number of phase rotation vectors and by applying point multiplication instead of matrix multiplication, giving a very light computational complexity, furthermore when it is combined with clipping gives the best of all result. Based on the result analyzed it can be concluded that clipping above 85% of peak value with preprocesses signal CCDF can be reduced marginally with least computational complexity and BER.

5. ACKNOWLEDGEMENT

Authors would like to present a greater-gratitude to Pune Institute of Computer Technology for providing resources and Principal Dr. P. T Kulkarni, HoED Dr. S.V. Gaikwad, for their motivation and Support. A special Thanks to Mr. Rajnarayan Shriwas for proofreading.

6. REFERENCES

[1] Anurag Kumar, D.Manjunath, Joy Kuri “Wireless Networking” Elsevier Morgan Kaufman publisher ISBN 0123742544 2008, pp 45-47, **2008**

[2] Ramjee Prasad “OFDM for Wireless Communications Systems” British Library ISBN 1580537960 PP 11-15, **2004**

[3] John G Prokies **2008**"Digital Communication" fifth edition Mcgraw Hills Publication ISBN 978–0–07–295716–7 PP 746-756

[4] Seung Hee Han and Jae Hong Lee, **2005**"An overview of peak-to-average power ratio reduction techniques for multicarrier transmission," in IEEE Wireless Communications, vol. 12, no. 2, pp. 56-65 doi: 10.1109/MWC.2005.1421929 April.

[5] Deepali Suresh Pawar Hemant S. Badodekar,**2018**" Review of PAPR Reduction Techniques in Wireless Communication," 2018 IEEE Global Conference on Wireless Computing and Networking (GCWCN), 978-1-5386-5201-5/18

[6] H. Arslan, **2007**, "CR, Software Defined Radio, and Adapt Wireless Sys," ISBN 978-1-4020-5542-3, Springer PP. 325–353,

[7] Yomo, Hiroyuki & Nguyen, Huan & Kyritsi, Persefoni & Duc Nguyen, Tien & S. Chakraborty, Shyam & Prasad, Ramjee, **2015**"PHY and MAC performance evaluation of IEEE 802.11a WLAN over fading channels". IETE Journal of Research. 51. 10.1080/03772063.2005.11416381.

[8] Sanjay Singh, M Satish Kumar, H.S. Mruthyunjaya,**2009,** "Effect of Peak to Average Power Ratio Reduction on the Multicarrier Communication System Performance Parameters," World Academy of Science, Engineering and Technology, 52, pp.1115-1122.

[9] Alexander M. Wyglinski, Maziar Nekovee, and Y. Thomas Hou, **2010**,"Cognitive Radio Communications and Networks Principles and Practice" ELSEVIER Inc, ISBN 978-0-12-374715-0 PP 63-64,

[10] M. Mounir, M. I. Youssef, and I. F. Tarrad,**2017,** "On the effectiveness of deliberate clipping PAPR reduction technique in OFDM systems," Japan-Africa Conference on Electronics, Communications and Computers (JAC-ECC), Alexandria, 2017, pp. 21-24.

[11] D. Levy, A. Reichman, and D. Wulich, **2018,** "Peak to Average Power Ratio Reduction for Filter Bank Multicarrier Modulation using Iterative Clipping and Filtering," 2018 IEEE International Conference on the Science of Electrical Engineering in Israel (ICSEE), Eilat, Israel, pp. 1-3.

[12] X. Liu, X. Zhang, J. Xiong, F. Gu, and J. Wei,**2019,** "An Enhanced Iterative Clipping and Filtering Method Using Time-Domain Kernel Matrix for PAPR Reduction in OFDM Systems," in IEEE Access, vol. 7, pp. 59466-59476,.

[13] Insu Sohn and S. C. Kim,**2015,** "Neural Network-Based Simplified Clipping and Filtering Technique for PAPR Reduction of OFDM Signals," in IEEE Communications Letters, vol. 19, no. 8, pp. 1438-1441

[14] Y. Aimer, B. S. Bouazza, S. Bachir, and C. Duvanaud, **2018,** "Evaluation of PAPR reduction based on block interleaving method in the presence of nonlinear PA model with memory," 25th International Conference on Telecommunications (ICT), St. Malo, 2018, pp. 451-455.

[15] Y. Aimer, B. S. Bouazza, S. Bachir, and C. Duvanaud, **2018,** "PAPR Reduction Performance in WiMAX OFDM Systems using Interleavers with Downward-Compatibility," 2018 IEEE International Symposium on Circuits and Systems (ISCAS), Florence, pp. 1-5.

[16] S. Al-Suhail, A. Ali and T. Al Naffouri,**2015,** "Peak-to-average power ratio reduction in interleaved OFDMA systems," 2015 International Symposium on Signal Processing and Info Tech (ISSPIT), Abu Dhabi, pp. 658-662.

[17] A. A. Eltholth and I. Atef, **2014,** "Chaotic Interleaving scheme for PAPR reduction in Cognitive Radio Systems," IEEE (APCWM) Bali, 2014, pp. 172-176.

[18] S. Wei, H. Li, G. Han, W. Zhang, and X. Luo,**2019**, "PAPR reduction of SLM-OFDM using Helmert sequence without side information," 2019 14th IEEE Conference on Industrial Electronics and Applications (ICIEA), Xi'an, China, pp. 533-536.

[19] V. Sudha, B. Anilkumar, M. S. Samatha, and D. S. Kumar, **2015**, "A low-complexity modified SLM with new phase sequences for PAPR reduction in OFDM system," Annual IEEE India Conference (INDICON), New Delhi, 2015, pp. 1-5.

[20] H. Liang, K. Chou, and H. Chu, **2017**,"A modified SLM scheme with two-stage scrambling for PAPR reduction in OFDM systems," 2017 IEEE 8th International Conference on Awareness Science and Technology (iCAST), Taichung, pp. 215-218.

[21] M. Rahman, M. S. Rahim, N. A. S. Bhuiyan and S. Ahmed, **2015,** "PAPR reduction of OFDM system using condex matrix-based SLM method with low computational overhead," Second Intern. Conf. on Electrical Information and Communication Technologies (EICT), Khulna, 2015, pp. 294-297.

[22] S. Ku, **2016**"An improved low-complexity PTS scheme for PAPR reduction in OFDM systems," IEEE International Conference on Signal Processing, Communications and Computing (ICSPCC), Hong Kong, 2016, pp. 1-5.

[23] M. Wang, J. Xiao, C. Yuan, Y. Tian and L. Zhang, **2017,**"A new low-complexity subblock segmentation method for PTS OFDM," IEEE 2nd Advanced Information Techn., Electronic and Automation Control Conference (IAEAC), Chongqing, 2017, pp. 2408-2411.

[24] K. Lee, Y. Cho, J. No, and D. Lim, **2016,**"A low-complexity PTS scheme using adaptive selection of dominant time-domain samples in OFDM systems," URSI Asia-Pacific Radio Science Conference (URSI AP-RASC), Seoul, 2016, pp. 1897-1900.

[25] Y. Cho, K. Kim, J. Woo, K. Lee, J. No, and D. Shin, **2017,**"Low-Complexity PTS Schemes Using Dominant Time-Domain Samples in OFDM Systems," in IEEE Transactions on Broadcasting, vol. 63, no. 2, pp. 440-445

[26] M. Akurati, Y. Kamatham, S. K. Pentamsetty, and S. P. Kodati, **2019,** "Reduction of PAPR in OFDM using Hybrid SLM-Companding for future Wireless Communications," Global Conference for Advancement in Technology (GCAT), BENGALURU, India, 2019, pp. 1-5.

[27] T. Sravanti and N. Vasantha, **2017,** "Performance analysis of precoded PTS and SLM scheme for PAPR reduction in OFDM system," 2017 International Conference on Innovations in Electrical, Electronics, Instrumentation and Media Technology (ICEEIMT), Coimbatore, , pp. 255-260.

[28] G. Rashwan, S. Kenshi, and M. Matin, **2017**"Analysis of PAPR hybrid reduction technique based on PTS and SLM," IEEE 7th Annual Computing and Comm. Workshop and Conference (CCWC), Las Vegas, NV, pp. 1-4